IV International Conference on Particle-based Methods – Fundamentals and Applications
PARTICLES 2015
E. Oñate, M. Bischoff, D.R.J. Owen, P. Wriggers & T. Zohdi (Eds)

PARAMETRIC EVALUATION FOR POWDER FLOWABILITY USING A FREEMAN RHEOMETER: A DISCRETE ELEMENT METHOD STUDY

Z. YAN, S. K. WILKINSON, S. A. TURNBULL, E. H. STITT, AND M. MARIGO

Johnson Matthey Technology Centre
PO Box 1, Belasis Avenue, Billingham, Cleveland, TS23 1LB, UK
E-mail: Michele.Marigo@matthey.com; web page: http://www.matthey.com

Key words: FT4 rheometer, Powder Flow, Discrete Element Method, Multisphere,

Abstract. A discrete element method (DEM) using the Hertz-Mindlin and JKR models was used to model the flowability measurement on a cohesive particulate material in the Freeman FT4 powder rheometer. An assessment of DEM parameterswas carried out to understand the operation of this equipment and to study the correlation between inter-particle properties and flowability. Simulation results indicate that the static and rolling friction coefficients, and JKR cohesion energy density are all negatively correlated with powder flowability, meaning that an increase in any of these parameters results in a decrease in powder flowability. At higher level friction, the force and torque have a larger measurement deviation, which is possibly due to local jamming in the particle bed. The powder flowability decreases as particle size increases for the current coarse grained system. Particles size distribution width has very little effect on the flowability changes. Particles with lower sphericity tend to have lower flowability possibly due to particle interlocking. It was demonstrated that rolling friction has a large effect on flowability for a give non-spherical particle shape.

1 INTRODUCTION

Flowability is the ability of granular media and powders to flow, and can influence the process performance during powder handling, including hopper discharge, powder feeding, blending, mixing, and die filling. Additionally, this can influence product quality. Flowability depends on multiple physical properties (for example: particle size, particle size distribution, shape factors, and surface texture) and environmental variables (temperature, humidity, pressure, etc.) [1, 2]. Recently, the Freeman FT4 powder rheometer (Freeman Technology, Malvern, UK) has become an increasingly popular device for measuring the flow energy of particulate materials. The characterisation consists of a dynamic test regime, in which the flow resistance encountered for an impeller moving within a powder bed is assessed.

Currently, the FT4 is commonly used for comparative studies and ranking of powder flow properties, but not yet as a quantitative support tool for process design or a possible calibration tool for DEM simulation [3]. Bharadwaj et al. [4] studied the effects of particle size, shape, size distribution and friction on force and torque on the impeller in the FT4. In this work non-cohesive glass beads were used to understand the operation of the FT4 in conjunction with a discrete element method (DEM). Hare et al. [5] showed in DEM simulations for cohesive salinized glass beads that measured torque had the biggest impact on flow energy measurement in the FT4. Following this literature precedent, the objectives of this paper are thus:

(1) To carry out a broader investigation using DEM for a better understanding on the FT4

operation.

(2) To investigate how input DEM interparticle properties govern the bed bulk response during the downward cycle for the dynamic test. This includes:
- Particle-particle properties such as static and rolling friction coefficients and cohesion energy density.
- Particle geometrical factors such as particle size, particle size distribution (PSD), shape.

2 METHODS AND PROCEDURES

2.1 Discrete Element Method (DEM)

In this work, the soft-sphere DEM approach developed by Cundall and Strack [6] using the Hertz-Mindlin contact model [7, 8] was utilised to calculate the normal and tangential contact forces. Cohesion of particles was modelled with the Johnson-Kendall-Roberts (JKR) model [9]. An additional term $\boldsymbol{F}_{coh}= k\mathrm{A}$ was added to normal contact force, where A is the particle contact area; k is the cohesion energy density in J/m^3 [10].

The FT4 DEM simulations were carried out using the open source DEM code, LIGGGHTS [11].

2.2 Description of the FT4

The FT4 measures the axial force and torque on the impeller blade that is rotated and moved downwards and upwards through the powder bed [12]. The force and torque reflect the resistance to powder flow.

The total flow energy is defined as the sum of the work done by both the axial and rotational motions of the impeller, given by [5],

$$\text{Flow Energy} = \int_0^h \left(\frac{T}{R\tan\alpha} + F\right) dh \tag{1}$$

where T is the torque on impeller blade; R is the radius of the impeller and α is the helix angle of impeller movement; F is the downward force acting on the blade; h is the vertical travel distance of impeller through the powder bed. The flow energy measured during the downward movement was utilised for the comparisons whereas it is assumed that low energy represents good flowability and conversely a high energy value represents poor flowability.

2.3 DEM input parameters

The FT4 equipment has the vessel made of borosilicate glass while the impeller blade was made of stainless steel. The DEM material property inputs for these were selected from the literature and are listed in the Table 1. While interaction between particle and walls such as restitution and friction between particles and the walls (blade and vessel) may have an effect on the bulk flow behaviour, the other material and wall properties were held constant and assigned with nominal ‘guessed’ values. This was done in order to reduce the numbers of varied parameters and consequently, simulations. In support of this assertion it is noted that Bharadwaj et al. [4] reported that the static and rolling friction between particle and wall have a much weaker impact compared with inter-particle friction in the DEM simulations of the FT4 using glass beads. Inter-particle properties such as inter-particle particle static ($\mu_{s\text{-}pp}$) and rolling ($\mu_{r\text{-}pp}$) friction coefficients, and cohesion energy density (k_{pp}) were varied to investigate their effect on the powder flow.

Table 1: DEM input parameters. Underlined the ones varied in this study.

Material parameters	Symbols	Values	Refs.
Young modulus vessel (GPa)	E_v	64	[4]
Young modulus blade (GPa)	E_b	190	[13]
Young modulus particle (GPa)	E_p	0.02	
Poisson's ratio vessel (-)	ν_v	0.25	[4]
Poisson's ratio blade (-)	ν_b	0.30	[13]
Poisson's ratio particle (-)	ν_p	0.2	
Particle density (kg/m^3)	P	2500	
Coefficient of restitution particle-blade (-)	ε_{pb}	0.7	
Coefficient of restitution particle-vessel (-)	ε_{pv}	0.7	
Coefficient of restitution particle-particle (-)	ε_{pp}	0.85	
Static friction coefficient particle-blade (-)	$\mu_{s\text{-}pb}$	0.30	
Static friction coefficient particle-vessel (-)	$\mu_{s\text{-}pv}$	0.30	
Static friction coefficient particle-particle (-)	$\mu_{s\text{-}pp}$	<u>0.05-0.50</u>	
Rolling friction coefficient particle-blade (-)	$\mu_{r\text{-}pb}$	0.05	
Rolling friction coefficient particle-vessel (-)	$\mu_{r\text{-}pv}$	0.05	
Rolling friction coefficient particle-particle (-)	$\mu_{r\text{-}pp}$	<u>0.05-0.45</u>	
Cohesion energy density particle-blade (J/m^3)	k_{pb}	50	
Cohesion energy density particle-vessel (J/m^3)	k_{pv}	50	
Cohesion energy density particle-particle (J/m^3)	k_{pp}	<u>10-10^5</u>	

Due to the computational power limitations, a grain-coarsening scheme was used to reduce particle number and increase time step in this study, in the same manner as reported by other researchers [4]. Spheres ranging from 0.6 to 3mm were used in this study.

2.4 Multi-sphere (MS) approach

It is commonplace in DEM simulations to represent non-spherical shapes using the multi-sphere method wherein the non-spherical particles are approximated by conjoining multiple spheres and integrating them as one rigid body [14]. In this study the effect of particle shapes was investigated by looking at particle sphericity. Sphericity (Φ_s) is defined as $\Phi_s = \pi^{1/3}(6V_p)^{2/3}/A_p$, where V_p is the volume of the object, A_p is its surface area [15].Table 2 reports the details about the MS clumps used in this investigation.

They consist of monosized small spheres, with the same volume equivalent diameter (d_v =3 mm), but differing in sphericity values. V_p and A_p were calculated by assuming that a MS clump has an ideal shape. V_p and A_p were calculated by assuming that a MS clump has an ideal shape. For example, for a cube clump V_p=a^3 and A_p=6a^2.

Table 2: Characteristics of the MS clumps. *N* is the total number, and d_0 is the diameter of the constituent spheres.

Shapes	Geometry (ideal shape)	MS clumps	Size (mm)	N	d_0 (mm)	Φ_s
Sphere	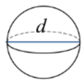		d = 3.0	1	3.0	1.0
Cylinder			l =2.620 H=2.620	27	0.874	0.87
Cube	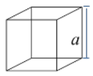	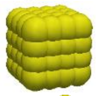	a=2.418	64	0.644	0.81
Tetrahedron	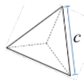		c=4.932	56	0.940	0.67

2.5 DEM simulation procedures

Prior to a test in the FT4, a conditioning preparation was conducted to ensure the particle bed have a reproducible initial condition [12]. Several repeat tests on monosized spherical particles at $\mu_{s\text{-}pp}$ = 0.50, $\mu_{r\text{-}pp}$ = 0.45, and k_{pp} =10^5 J/m^3 were carried out first. This test condition was expected to have the worst powder flowability for the parameter range selected (shown in the following sections), and might experience particle-bridging during natural packing under gravity. Additionally, a flow energy change due to particle rearrangement was expected after conditioning. However, it was shown that the conditioning stage has a negligible effect on the calculation for the flow energy. Therefore for all simulations with spherical particles, the conditioning step was ignored to reduce the central processing unit (CPU) time cost; a decision corroborated by other publications [4]. For simulations with non-spherical particles, the clumps consist of too many fine constituent particles, which make the computation even more CPU and time consuming. Thus the conditioning stage was also ignored. During the test cycle, the impeller moves downwards whilst being rotated anticlockwise with a helix angle of 5^o and a tip speed of 100 mm/s.

3 PARAMETRIC STUDIES

3.1 Effect of static and rolling friction

Fig. 1 plots the force (Fig.1a) and torque (Fig.1b) on the blade, and the resultant flow energy (Fig.1c) via Eq. (1) for different friction levels. It is seen that, compared with the baseline test ($\mu_{s\text{-}pp}$ = 0.05, $\mu_{r\text{-}pp}$ = 0.05), an increase in rolling friction coefficient ($\mu_{s\text{-}pp}$ = 0.05, $\mu_{r\text{-}pp}$ =0.45) seems to have very little effect on the force, but a very significant effect on the torque. Therefore torque, compared with force, is more sensitive to rolling friction, which implies that flow resistance to rotational motion of blade is larger than to axial motion [4]. An increase in static friction coefficient ($\mu_{s\text{-}pp}$ = 0.50, $\mu_{r\text{-}pp}$ =0.05) has a significant effect on both the force and torque, resulting in an increase in flow energy. Force and torque at a high level of static friction show larger deviation than at a high level of rolling friction, possibly due to the local jamming of the powder as the blade is subject to higher flow resistance. On an average basis, static friction has a major contribution to flow resistance, and rolling friction has a lesser one. A more rigorous method combining Design of Simulations (DoS) and

Principal Component Analysis (PCA) is currently being developed to study the parameter sensitivity in greater detail.

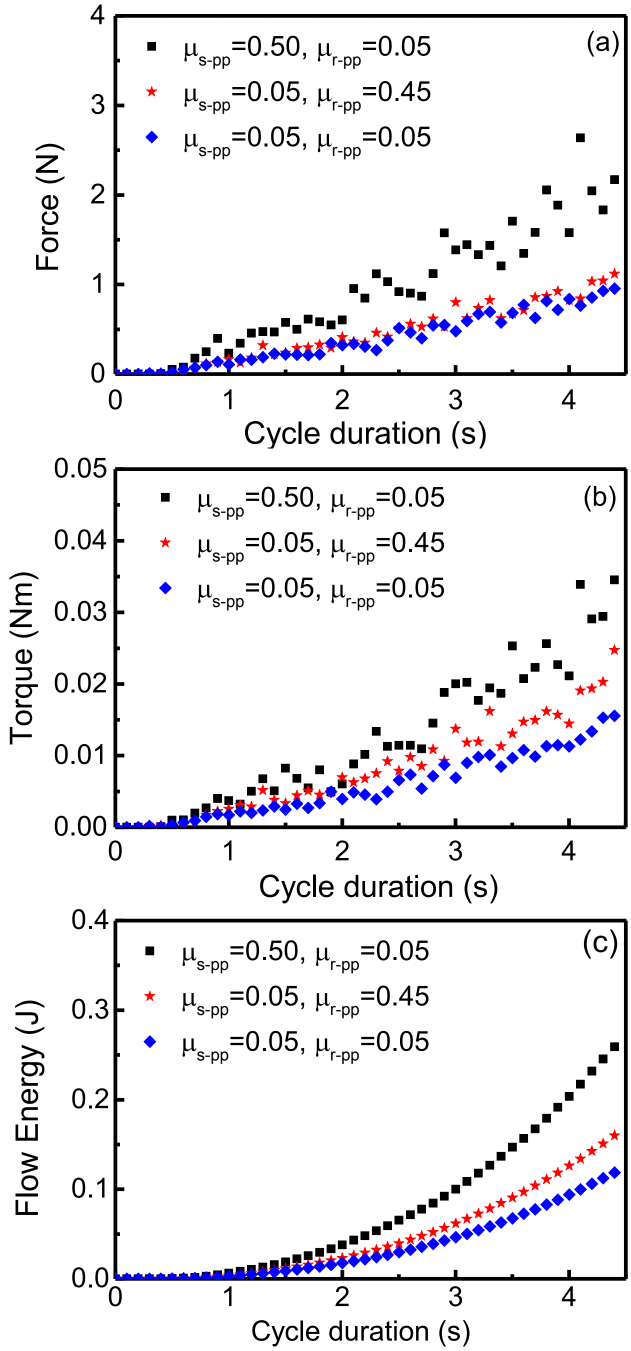

Figure 1: The force, torque on blade and flow energy during test cycle with spherical monosized particles (2mm in diameter). Conditions: E_p=0.02GPa, ε_p=0.85, and k_{pp}=10^5 J/m^3

3.2 Effect of cohesion energy density

Fig. 2 shows the effect of the cohesion energy density. It is seen that at the low level of static and rolling friction, the effect of cohesion energy density is small on calculated flow energy, while its effect is more significant at a high level of static and rolling friction. This suggests that cohesion energy and the friction are positively cross-correlated. The interaction of these parameters is something which will require further scrutiny through design of simulations (DoS) and sensitivity analysis approaches.

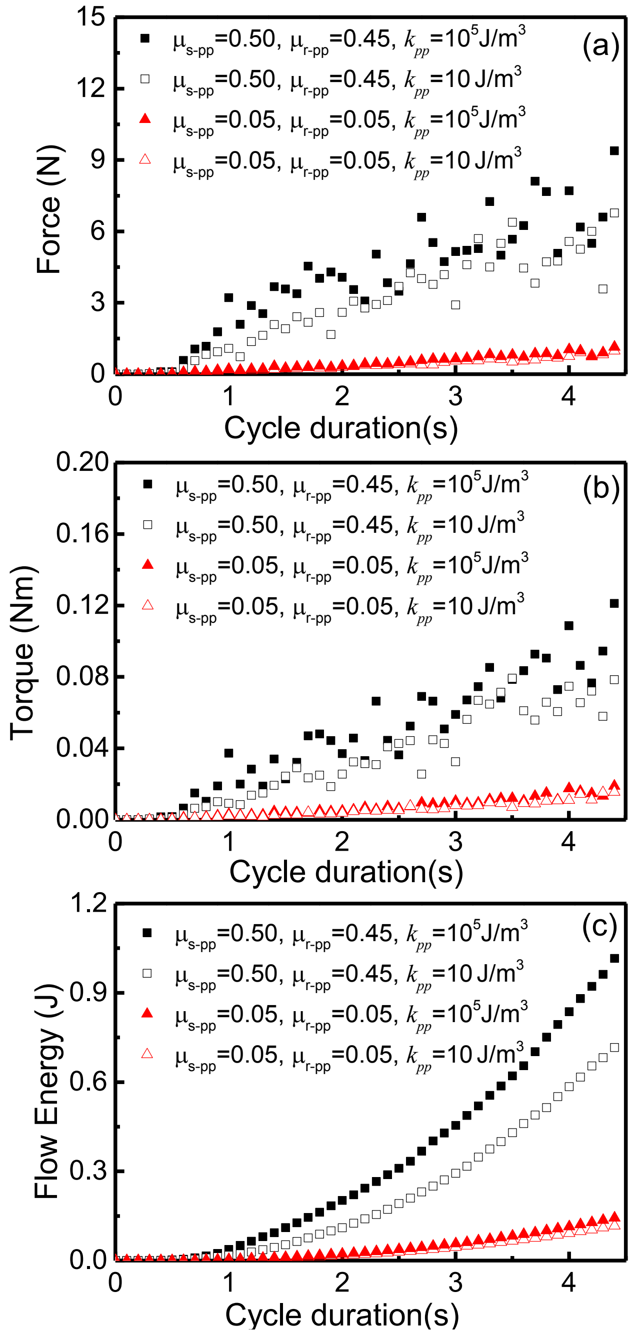

Figure 2: The force, torque on blade and flow energy during test cycle with spherical monosized particles (2mm in diameter). Conditions: E_p=0.02GPa, and ε_p=0.85.

3. 3 Effect of particle size

Fig. 3 shows the effect of particle size on the force, torque and flow energy measurement. It shows that the force and torque increase as the particle size increases. Bharadwaj et al. [4] found the same trend with non-cohesive glass beads in DEM simulations. Experimental data in [16] shows that, for a cohesive powder, cohesivity increases as particle size decreases. This is due to smaller sized powders having larger contact areas, resulting in lower flowability. Other inter-particle forces such as van der Waals and electrostatic forces also contribute to the size dependency of flowability for fine powder. However, the role of such forces was not considered in this study. Thus, the simulations in this study are not comparable with experimental observations of fine, cohesive materials. In this coarse-grained cohesive system, the flowability of powder decreases as the particle size increases. This is possibly because the effect of the cohesion energy density, at the chosen value in this study, was not prominent in a coarse-grained system. Liu et al. [17] found the flowability of pulverised coal (40-240 μm) decreased as its mean size increased in the FT4 basic flow energy. However, in their measurement the cohesivity of the coal was unknown. Fine particles need to be considered and more comprehensive contact models should be included.

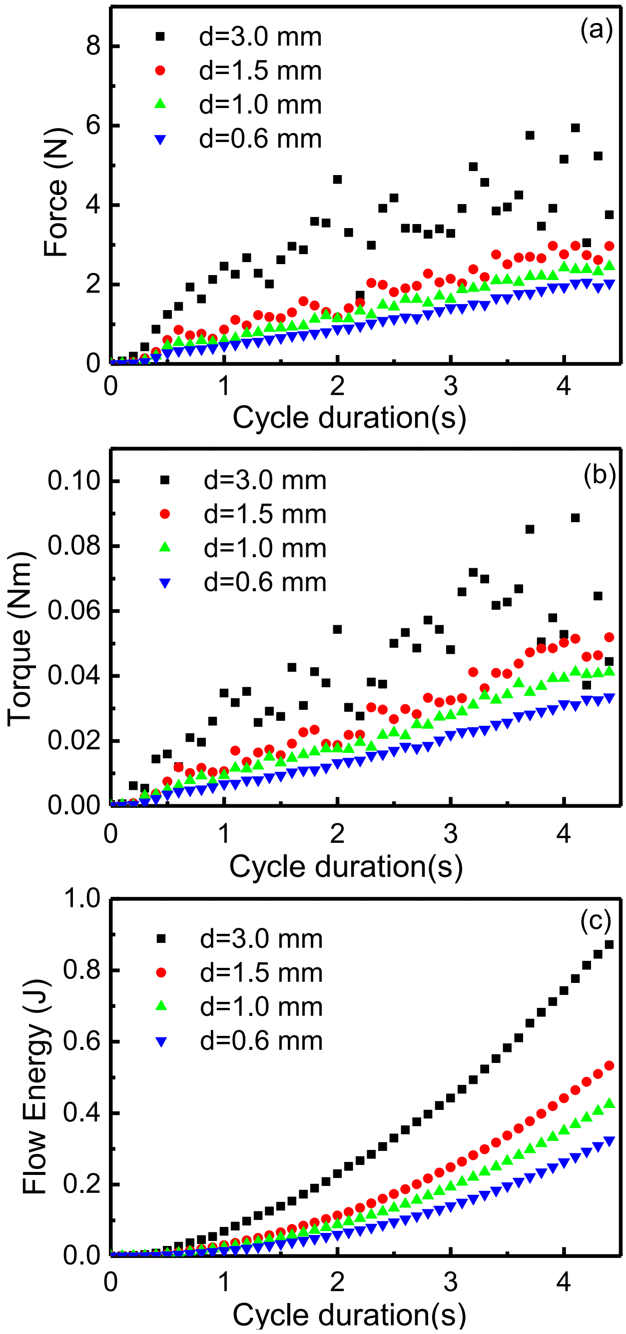

Figure 3: Effect of particle size on the force, torque and flow energy. Conditions: E_p=0.02GPa, ε_p=0.85, and k_{pp}=10^5 J/m^3

3. 4 Effect of particle size distribution (PSD)

Powders with PSD (number based) in a normal distribution $f(d) = \frac{1}{\sigma\sqrt{2\pi}} \exp(-\frac{(d-d_0)^2}{2\sigma^2})$ were modelled in this this study. The powders have the same mean size d_0 = 2 mm but with different distribution standard deviation (σ=0, 0.2, 0.4 and 0.6). Smaller σ value means a narrower PSD (specially, σ=0 for monosized powder). Particles under 600 μm (diameter) were cut off as presence of a lot of fine particles is CPU and time costly. Fig. 4 shows the PSD effect on force, torque and flow energy during the test cycle. It seems in this study, the particle size distribution width has a very small effect on flow resistance. This indicates that the uncertainties in the PSD within the current range would not significantly affect the force, torque and flow energy. For cohesive powders, a broader PSD will impede flowability. This is due to the fact that a powder with differently sized particles enables more efficient particle packing. A higher packing density leads to an interlocking effect as the small particles fill in the gaps between larger ones. Also the higher contact surface area is expected to contribute larger cohesive force [18]. For particles with a number based normal distribution, the volume fraction of the small particles is rather low. Furthermore, the fine particles (under 600μm) were discounted for the aforementioned reason. For these two reasons, the difference in total contact the surface area is not prominent for different σ values, explaining an insignificant of effect of PSD on flowability. However, for the sample with monosized particles, force, torque and flow energy were slightly lower than for samples having a normal distribution in particle size.

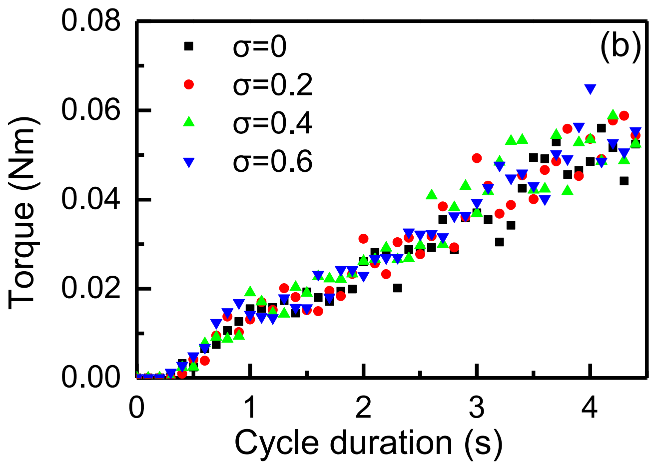

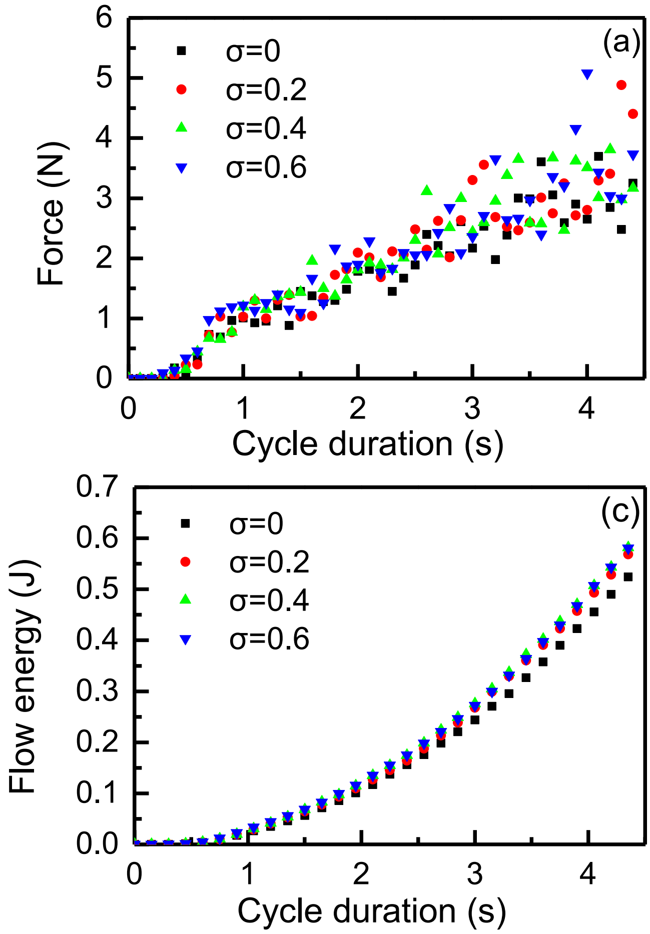

Figure 4: Effect of particle size distribution on the force, torque and flow energy. Conditions: E_p=0.02GPa, ε_p=0.85, and k_{pp}=10^5 J/m^3

3. 5 Effect of shape factors

Fig. 5 plots the results for the bed material consisting of different shaped clumps (see Table 2); showing the increase in force, torque and flow energy as the sphericity of the clumps decreases. Considering that the clumps have the same volume equivalent size d_v, it was presumed that the difference in measurements is not due to the difference in clump size (as shown in Section 3.3 where particle size has an effect) but in the sphericity. Generally, the sphericity of the particles represents the rolling resistance of the particles; the more angular the clump, the larger the rolling resistance, and hence the lower the flowability of the powder. Cleary et al. [19] and Santos et al. [20] both found a lower sphericity of irregular shaped particles led to lower flowability of powders. Furthermore, when the rolling friction was also considered for the clumps, it was seen that the presence of rolling friction can play an extra contribution to the decrease of flowability. Markauskas et al. [21] found both the shape factor and rolling friction should be considered to model the flow behaviour of the irregular shaped powders in a hopper.

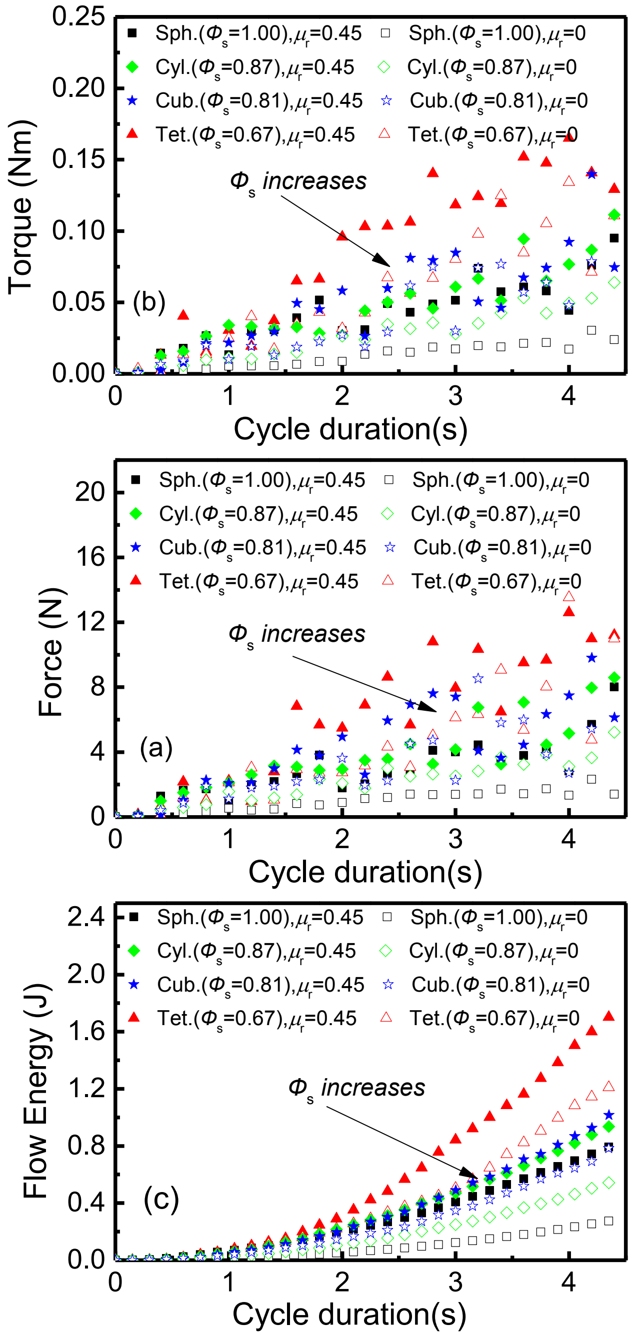

Figure 5: Effect of sphericity of non-spherical particles on the force, torque and flow energy. Conditions: E_p=0.02GPa, ε_p=0.85, and $k_{pp}=10^5$ J/m^3

4. CONCLUSIONS

A DEM approach was used to model the flowability of a cohesive powder in the FT4 powder rheometer. A parametric study was carried out to investigate the effect of inter-particle properties such as inter-particle static and rolling friction coefficients, cohesion energy density, particle size, size distribution, and shape factors on flowability in a coarse-grained system. The important findings are as follows:

- An increase of the particle-particle static or rolling friction coefficients, or cohesion energy density, leads to increase of the force and torque on the blade and flow energy, indicating a decrease of the flowability of powder. At a high level of friction, the force and torque have larger measurement deviation, possibly because of local jamming the material bed. Friction coefficients and the cohesion energy density are positively cross correlated.

- In the current coarse-grained system, the flowability of particles decreases as particle size increases. Conversely, a lower flowability for finer powders was observed in experiments from the cited literature. This is due to the fact that other interparticle force effects, playing a role for finer real particles, are not considered in this DEM model.
- Particle with a normal distribution in particle size shows lower flowability than that with monosized particles; however, it seems that the particle distribution width has a very small effect on flowability change. This might be due to the volume faction of smaller particles is rather low for a number based normal PSD in all the simulations and the contribution of the increased surface area is not prominent.
- A multisphere approach was used to account for the irregular shape of particles by approximating them as rigid clumps. A powder whose particles have lower sphericities tends to have lower flowability due to a mechanism of particle interlocking. It is also shown that rolling friction should be also incorporated to better predict the flowability of a powder with irregular shapes.

The current proposed DEM has been used to investigate the operation for the FT4 rheometer during the downward cycle. Further work is being carried out to understand:

- The effect of input parameter sensitivity and interactions by using a more rigorous method combining Design of Simulations (DoS) and Principal Component Analysis (PCA) similarly to the one developed in Ref. [22].
- The inclusion of fine particles and experimental validation to verify the current DEM and grain coarsening scheme.
- The effect of segregation due to particle size effects.

5. ACKNOWLEDGMENTS

This work is supported by the IPROCOM Marie Curie initial training network, funded through the People Programme (Marie Curie Actions) of the European Union's Seventh Framework Programme FP7/2007-2013/ under REA grant agreement No. 316555.

6. REFERENCES

[1] Ganesan, V., Rosentrater, K.A., and Muthukumarappan, K. Flowability and handling characteristics of bulk solids and powders - a review with implications for DDGS. Biosyst. Eng. (2008)101:425-435.

[2] Yang, S., and Evans, J.R.G. Metering and dispensing of powder; the quest for new solid freeforming techniques. Powder Tech. (2007)178:56-72.

[3] Pantaleev S, Yordanova S, Ooi J., and Marigo M. Powder Mixing - an Experimentally Validated DEM Study Joint 5th UK-China & 13th UK Particle Technology Forum, 13rd-15th 2015, Leeds, UK.

[4] Bharadwaj, R., Ketterhagen, W.R., and Hancock, B.C. Discrete element simulation study of a Freeman powder rheometer. Chem. Eng. Sci. (2010) 65:5747-5756.

[5] Hare, C., Zafar, U., Ghadiri, M., Freeman, T., Clayton, J., and Murtagh, M. Analysis of the Dynamics of the FT4 Powder Rheometer. Powder Tech. (2015) doi:10.1016/j.powtec.2015.04.039
[6] Cundall P.A, Strack O.D.L. A discrete numerical model for granular assemblies. Geotechnique (1979) 29:47-65.
[7] Hertz H. Ueber die Berührung fester elastischer Koerper. J. Reine Angew Math. (1881) 92: 156-171.
[8] Mindlin R.D. Compliance of elastic bodies in contact. ASME Trans. J. Appl. Mech. (1949) 16: 259-268.
[9] Johnson, K.L., Kendall, K., and Roberts, A.D. Surface energy and the contact of elastic solids. Proc. Math. Phys. Eng. Sci. (1971) 324:301-313.
[10] Grima, A.P., and Wypych, P.W. Development and validation of calibration methods for discrete element modelling. Granul. Matter (2011)13:127-132.
[11] Kloss, C., Goniva, C., Hager, A., Amberger, S., and Pirker, S. Models, algorithms and validation for opensource DEM and CFD-DEM. Prog. Comput. Fluid Dy. (2012) 12:140-152.
[12] http://www.freemantech.co.uk
[13] An, Z., Ying, A., and Abdou, M. Application of discrete element method to study mechanical behaviors of ceramic breeder pebble beds. Fusion Eng. Des. (2007) 82:2233-2238
[14] Amberger, S., Friedl, M., Goniva, C., Pirker, S., and Kloss, C. Approximation of objects by spheres for multisphere simulations in DEM. In ECCOMAS 2012, 10-14 Sept., 2012,Vienna, Austria
[15] Wadell, H. Volume, Shape and Roundness of Quartz Particles. J. Geology (1935) 43: 250-280.
[16] Hou, H., and Sun, C.C. Quantifying effects of particulate properties on powder flow properties using a ring shear tester. J. Pharma. Sci. (2008) 97:4030-4039.
[17] Lu, H., Guo, X., Liu, Y., and Gong, X. Effect of Particle Size on Flow Mode and Flow Characteristics of Pulverized Coal. KONA Powder Part J. (2015) 32:143-153
[18] Xu X., Yao, S., Han, N. and Shao B. Measurement and influence factors of the flowability of microcapsules with high-content β-carotene. Ch. J. Chem. Eng. (2007) 15:579-585.
[19] Cleary, P.W., and Sawley, M.L. DEM modelling of industrial granular flows: 3D case studies and the effect of particle shape on hopper discharge. Appl. Math. Model (2002)26:89-111.
[20] Dos Santos, E.G., da Silva Carvalho, L.C., Mesquita, A.L.A., Mesquita, A.L.A., and Gomes, L.M. A study about the particle shape effect using the discrete element method (DEM). 15th Brazillian Congress of Thermal and Enginering, 10-13, Nov., Belem, PA, Brazil
[21] Markauskas, D., and Kačianauskas, R. Investigation of rice grain flow by multi-sphere particle model with rolling resistance. Granul. Matter (2011)13(2):143-148.
[22] Yan Z., Wilkinson S.K., Stitt E.H., and Marigo M., Discrete Element Modelling (DEM) input parameters: understanding their impact on model predictions using statistical analysis, Computational Particle Mechanics (2015) (under review).